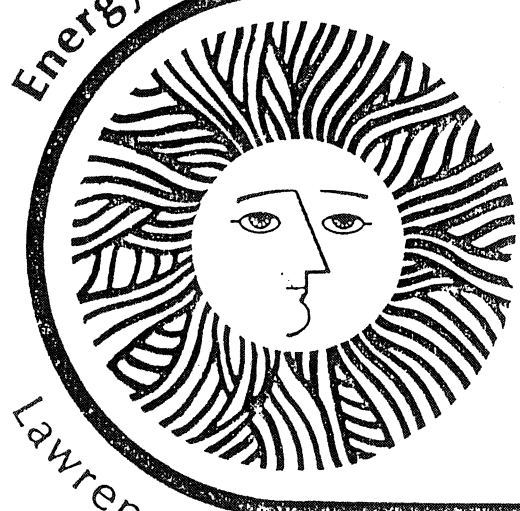


*To be presented at the Air Infiltration Symposium,
at the Annual Meeting of ASHRAE, Philadelphia,
Penn., January 30, 1979 and to be published in
ASHRAE Transactions 1979, Vol. 85, Part I.*

Energy and Environment Division



**Infiltration — Pressurization
Correlations: Detailed Measurement
on a California House**

*D.T. Grimsrud, M.H. Sherman,
R.C. Diamond, P.E. Condon,
and A.H. Rosenfeld*

December 1978

Lawrence Berkeley Laboratory University of California/Berkeley
Prepared for the U.S. Department of Energy under Contract No. W-7405-ENG-48

LBL-7824

LBL-7824
EEB-Env-78-5

INFILTRATION--PRESSURIZATION CORRELATIONS:
DETAILED MEASUREMENTS ON A CALIFORNIA HOUSE*

D. T. Grimsrud, M. H. Sherman, R. C. Diamond
P. E. Cordon, A. H. Rosenfeld

Energy and Environment Division
Lawrence Berkeley Laboratory
University of California
Berkeley, California 94720

To be published in ASHRAE TRANSACTIONS 1979, Vol. 85, part 1.

* This work was supported by DOE, Assistant Secretary for Conservation and Solar Applications, Division of Buildings and Community Systems.

Abstract

Infiltration studies have been carried out in a typical tract home in the San Francisco Bay area. Houses in this region as a result of the mild climate are loosely constructed, and show large air leakage rates.

Infiltration rates of up to 1-1/4 air changes an hour were measured using a controlled flow tracer gas technique with nitrous oxide as the tracer gas. Air leakage rates were measured using fan pressurization of the house with a range of pressures from 7.5 to 75 Pascals. In addition to weather data taken on site, pressure sensors mounted on the exterior walls were critical in establishing a pressure model for air infiltration. Measured inside-outside pressure differences were less than a tenth of those expected based upon wind speed measurements made on site. Measurements also show significant (20%) duct leakage and air flow between the attic, living space and crawl space.

Keywords: Air-Flow, Air Leakage, Duct, Furnace, Modeling, Residential, Turbulence, Ventilation.

INTRODUCTION

Many measurements of infiltration rates in single family detached houses have been reported in the literature (see Ref. 1 for a review of these results). This paper describes infiltration studies in a single-family residence in a suburban setting, part of a larger study examining the correlation between infiltration and air leakage rates under fan pressurization in several California houses.

The motivation for seeking the correlation arises because of the wide range of results obtained by those who attempt to relate infiltration rates to weather parameters. While the dependences on wind and temperature are similar for measurements on different single-family residences, the constants which enter the equation differ widely from house to house. The major source of this variation may be the differences in construction quality and geometry between houses which determine the leakage detail of the structure. If this hypothesis is valid, an independent measurement of construction quality should reduce the variation between coefficients and allow adequate modeling of air infiltration rates for a small number of "typical" houses characterized by geometry alone.

How can construction quality be measured? Current thinking suggests that fan pressurization measurements of air leakage may provide the best measurements for purposes of air infiltration modeling. A pressure difference is achieved by temporarily sealing a fan to the building shell. Mass flow continuity then predicts that the air flow rate through the fan is equal to the air leakage rate of the structure at the working pressure difference. Fan pressurization measurements of air leakage are not analogs of natural infiltration because the pressure distributions on the building shell are quite different in the two cases. In the first, the pressure over the entire shell is quite uniform while in the second the pressures vary in a complicated manner both in space and in time. But measurements of air leakage in two structures using the same working pressure does allow one to compare the two structures. If this comparison can also be used to predict comparative air infiltration rates for the two structures (normalized to the same weather conditions) then the fan pressurization measurement will be very useful, indeed. Once sufficient data on infiltration rate vs weather conditions for typical housing styles have been determined, a single fan pressurization measurement in a specific house, requiring inexpensive equipment and a modest amount of time, could be used to determine the coefficients in the relationship of infiltration rate vs weather parameters for that house. This information could then be used with a typical weather record for a heating (or cooling) season to predict the amount of air infiltration for the season and the energy use and peak air conditioning power associated with that infiltration.

Inverting the process, knowledge of the heat load due to natural infiltration in houses of known air leakage should allow a standard to be written for the maximum air leakage in a house at a particular pressure when using fan pressurization.

There are many unverified assumptions associated with the statements made above. These must be examined carefully in each structure under investigation. In the house we have been investigating, we have found that surface pressure measurements are an essential step in attempting to understand the relationship between infiltration rate and local weather. Furthermore, they suggest that in heavily wind-shielded structures the pressure distribution on the building shell established by fan pressurization may be more closely related to the natural pressure distribution on the shell than was heretofore believed.

The importance of adequately understanding each structure under investigation cannot be overemphasized. In this house, furnace duct leakage is an important factor that complicates both measurements and interpretations. The possible generality of this result is therefore limited to the class of homes which use forced air heating ducts passing through unconditioned spaces.

DESCRIPTION OF THE TEST SITE

The Research House is located 20 miles east of San Francisco in Walnut Creek. Separated from the mild coastal climate by the Coast Range, Walnut Creek has a weather pattern typical of much of California. A rainy winter season with daily temperatures (24-hr period) ranging from 2°C (35°F) to 13°C (55°F) is followed by a dry summer season with daily temperatures ranging from 14°C (58°F) to 32°C (90°F). Winter design temperatures (99%) for the area is -4°C (24°F) and for the summer 38°C (100°F).

The house is a one-story, three-bedroom house, with wood frame construction, typical of houses in the area. Built in 1964, the house has whole-house-air conditioning, a forced-air gas heating system, with the heating ducts passing through the crawl space and return duct passing through the attic. The windows are single-glazed horizontal sliding windows with aluminum frames, and the walls are all insulated with R-11 fiberglass batts. Excluding the attic and crawl space, the house has a floor area of 100 m² (1080 ft²) and a volume of 230 m³ (8100 ft³).

Figure 1 shows a plan view of the house and its surroundings. Wind shielding by other houses, mature trees and fences is significant; we believe that this amount of shielding precludes any straight-forward modeling of the relationship between infiltration rates and local weather conditions.

AIR LEAKAGE MEASUREMENTS

The leakage of the house as a function of the indoor-outdoor pressure differences is shown in Fig. 2. These measurements were made by mounting a tubeaxial fan driven by a variable speed motor on a plywood panel and sealing this assembly into an open door frame. Adjusting the fan speed allows control of the indoor-outdoor pressure difference. This pressure difference was measured using a diaphragm pressure gauge which had been calibrated using a capacitance pressure sensor. Flow continuity demands that the air flow through the fan is equal to the air leakage of the structure under test. The air flow rate through the fan was measured using a flowmeter, which we calibrated using a Pitot tube traverse technique following the AMCA Standard Test Code for Air Moving Devices.

Also shown on Fig. 2 is the leakage of the house measured when the return air duct and the warm air register openings were covered with plastic and sealed with tape. Duct leakage of this magnitude is typical of the leakage seen in all the houses we have measured in this region.

AIR INFILTRATION MEASUREMENTS

Air infiltration rates have been measured using nitrous oxide as a tracer gas. Several techniques have been employed during various stages of this study. All the methods use an infrared gas analyzer to measure the concentration of the N₂O. The differences between the methods employed are in the techniques used to control the injection of the gas into the test space. A complete description of the apparatus is in the ASTM paper of Condon, et al. (2).

Initial measurements were made using an injection control strategy in which the tracer gas was on for an hr, off for an hr, on for an hr, etc. The injection and sampling ports were both mounted in the return duct of the furnace. The furnace blower circulates air through the house at a rate of 0.40 m³/s (850 cfm). This corresponds to approximately 6 air changes per hr in the house when the blower is operating.

When the injection rate is zero, the concentration changes with time according to the familiar relation.

$$C = C_0 e^{-At} \quad (1)$$

where C is the concentration at time t , C_0 is the concentration at $t = 0$ and A is the air exchange rate. Plotting the concentration as a function of time on semilog graph paper gives a straight line if A is constant. The negative of the slope of the line gives the air exchange rate.

Weather parameters were monitored at the site while the air exchange rates were being measured. The weather tower is mounted on the center of the garage roof; the cup anemometer is located 4.9 meters (16 ft) above the peak of the garage roof which is 4.3 m (14 ft) above the ground. Wind speed, wind direction and outdoor dry-bulb temperature were measured on this tower. In addition indoor air temperature and relative humidity were measured using a hygro-thermograph located near the center of the house.

Infiltration rates, taken during May, are plotted as a function of wind speed in Fig. 3. The number in parentheses by each data point is the indoor-outdoor temperature difference. The pressure differences due to the wind are, in principle, much larger than those due to temperature differences in the data sample we collected. However, careful analysis of the data showed that the small temperature differences seen during these measurements are also important in attempting to understand infiltration rates. The small pressures that are associated with these temperature differences suggest that small pressure differences should be associated with the wind, a most peculiar result. These observations suggest that the inference of infiltration rates directly from the weather data without the intermediate step of measuring actual surface pressures on the house is, at best, problematical.

SURFACE PRESSURE MEASUREMENTS

Surface pressures were measured at fourteen locations on the shell of the structure. Eight (on the walls) are indicated by X's in Fig. 4a. In addition, three probes were mounted in the attic to measure the pressure difference between the attic floor and the living space; three others were placed in the crawl space. A capacitance pressure sensor was used for the measurements. The sensor was modified to operate in a differential mode comparing the pressure of the inside of the house with that of one of the fourteen probes. The probes were connected to the sensor through a manifold which allowed the probes to be sampled sequentially for 1-min intervals. The sampling manifold was controlled by a microprocessor; the output of the pressure sensor was converted to a digital signal and stored by the same microprocessor.

The results of the pressure measurements are startling. A sample trace showing pressure as a function of time is shown in Fig. 4b. Often, all fourteen probes (including the probes measuring pressure differences across the ceiling into the attic and the floor into the crawl space) showed similar behavior. Pressures usually fluctuated about zero during each 1-min sampling period. This occurred even in conditions of a strong wind. The numbers by each tap location in Fig. 4a show an example of this. The average of the positive pressures and the average of the negative pressures observed during 1-min sampling periods are presented. The pressure at a tap was sampled once each sec for 1-min. The non-zero values of both positive and negative averages indicate the fluctuating nature of the surface pressures. The wind speeds, while these surface pressures were measured, ranged between 2 m/s (5 mph) and 16 m/s (35 mph) and averaged 8 m/s (18 mph). The wind was from the southwest.

Comparing the pressures in Fig. 4a with $1/2 \rho V^2 = 1/2(1.2)(8)^2 = 38$ Pa, the nominal pressure of an 8 m/s wind striking normal to a plane surface, shows that the surface pressures on the house are ten-fold smaller than $1/2 \rho V^2$ and have a significant fluctuating component. Therefore, models which attempt to predict infiltration in one-story houses with significant shielding from the wind must address pressure distributions of this kind.

MODELS

Air infiltration in buildings can be considered to be the result of the interaction between two separable factors: (a) the structure of the building envelope, and (b) the environment surrounding the envelope. In order to construct a model of the interaction several simplifying assumptions will be useful.

First, we assume that cracks allowing air flow through the shell are evenly distributed and indistinguishable. This assumption will cause errors if there are a small number of large

cracks (or leaks) in the envelope; however, large leaks are usually easy to find and to repair. Second, we assume that the pressure on the house can be modeled by using the local weather patterns, i.e. the weather measured by the weather tower on site, rather than the actual microclimate around the envelope. We comment further on this assumption below.

It is tempting to add a further assumption that only slowly varying components of the weather contribute to the infiltration. However, our measurements suggest that for this structure, and for many other structures in a heavily shielded environment, this assumption is not justified. In fact, fluctuating surface pressures appear to be the dominant mechanism driving air infiltration.

SHELL LEAKAGE

Infiltration losses can be estimated from the leakiness of the envelope and indoor-outdoor surface pressure difference. These pressure differences are related to the microclimate outside the structure which in turn is related to the local weather and the microenvironment. Therefore the pressure distributions around the house act to mediate the interaction between the local weather and infiltration. At every point on the surface, we define a leakage function $\ell(\Delta p, \vec{\sigma})$, where $\vec{\sigma}$ is the outwards normal vector, Δp is the pressure difference and ℓ is the leakage per unit area.

Several studies have examined the leakage function for a given crack size and type. A careful study by Honma (3) of laboratory models of cracks showed that the flow, Q , through a crack subjected to a pressure difference Δp can be represented by

$$Q = K d \Delta p^{1/\beta} . \quad (2)$$

In this expression, K is a proportionality constant describing the crack, and d is the length of the crack. The exponent β is also a function of Δp since flow through a crack is usually neither purely laminar (for which $\beta = 1$) nor fully developed turbulence (for which $\beta = 2$). Honma described the results of his measurements with the expression

$$\beta = 2.0 - \exp \{-A\Delta p\} . \quad (3)$$

Here A is an empirical constant which incorporates information about the crack. We observe that as Δp becomes small, β goes to unity while at large values of Δp , β approaches 2. It is interesting to note that for small pressures (less than 5 Pa) and for all cracks tested (widths of 1.05 mm and smaller) the exponent of flow, β , always had values less than 1.005 (very laminar flow).

In general, the crack distribution of the shell is unknown. From fan pressurization measurements of the air leakage of the shell we can find an average leakage function

$$Q = L(\Delta p) = [\phi \ell(\Delta p, \vec{\sigma}) dA] . \quad (4)$$

In this expression Q is the air leakage due to fan pressurization; the surface integral is simply the sum of the leakage function per unit area over the entire building shell.

Measurements of the Q as a function of Δp induced by the fan yield $L(\Delta p)$ in Fig. 2. The total area of the shell of the living space for this house is 300 m^2 .

SURFACE PRESSURES

If weather conditions in the vicinity of the building are known it is possible, in principle, to calculate surface pressure differences. These pressure differences are due to the temperature differences between indoor and outdoor air (stack effect) and the dynamic pressure caused by wind striking the surface of a wall. Many well-recognized uncertainties exist in calculating pressures due to both the stack effect and dynamic pressures. Our experience from the Walnut Creek research house demonstrates the importance of actual measurements of surface pressures. As indicated above, observations in this structure, heavily shielded from the wind, show surface pressures much smaller than expected with a large fluctuating component.

COMPUTATION OF INFILTRATION FROM PRESSURE MEASUREMENTS

Several models of flow due to surface pressure differences are possible. We shall suggest one and show later that it is consistent with measurements at this site. We make the following assumptions:

- (a) Complete mixing between indoor and outdoor air occurs when infiltrating air moves through the wall. Air movement along the wall of 10 ft/min (50 mm/s) sweeps incoming air emerging from a crack (width 1 mm) across that crack in about 0.02 sec. Therefore fluctuations of pressure having frequencies greater than 50 Hz would be required to prevent mixing.
- (b) The flow, Q , is equal to the leakage function $L(\Delta p)$, a slowly varying function of Δp (cf. Fig. 2 at 1/2 Pascal pressure).
- (c) No phase lag exists between the pressure differences and the resulting flow, (i.e., this is purely resistive flow).
- (d) The infiltration is equal to the exfiltration which is half the absolute value of all the air flow through the envelope.

In the pressure regime we are examining, the driving pressures are small. Therefore we assume a leakage function linear in Δp or

$$L(\Delta p) = K(\Delta p) \cdot \Delta p . \quad (5)$$

The air flow rate through the entire structure is then equal to the total infiltration which is the total flow resulting from the positive pressure differences on the building shell.

Thus, in the time interval T

$$Q = K(\Delta p) \times \overline{\Delta p} \quad (6)$$

where

$$\overline{\Delta p} = \frac{1}{T} \int_{-T/2}^{T/2} \max(0, \Delta p) dt \quad (7)$$

is the time average of the positive pressure on a surface. This average is computed by the same microprocessor that controls the pressure tap manifold in our experimental package.

CALCULATED FLOW

Measurements of the air leakage using fan pressurization (Fig. 2) permit us to estimate the air flow through the house when pressures are low. When the furnace ducts are open but the furnace blower is off we find

$$Q = 161 \overline{\Delta p} \quad (8)$$

where Q is given in m^3/hr and $\overline{\Delta p}$ is measured in Pascals. When the ducts are sealed we have

$$Q = 126 \overline{\Delta p} . \quad (9)$$

In general Q represents flow through all the openings of the shell. If we assume that the flow is dominated by flow through cracks we can expect that at small values of Δp , the flow is proportional to Δp while at high values it is proportional to $(\Delta p)^{1/2}$. Since the transition between the two flow regimes depends upon the crack dimensions, for an arbitrary value of Δp we expect that

$$Q = A(\Delta p)^{1/2} + B(\Delta p) . \quad (10)$$

It is tempting to fit curves such as Fig. 2 to such a function. However A and B are not constants but are themselves functions of the pressure difference. We therefore divide data such as that of Fig. 2 into three flow regimes:

- I Low pressure: $Q \propto \Delta p$
II Intermediate pressure: $Q \propto A(\Delta p)^{1/2} + B(\Delta p)$
III High pressure: $Q \propto (\Delta p)^{1/2}$

Examination of the data of Fig. 2 shows that the high pressure regime begins at about 45 Pa for this system. Data for pressures less than 45 Pa were fit to Eq. 10. The values of flow for $\Delta p = \pm 5$ Pa were then calculated from the equation; linear fits between ± 5 Pa were used to establish Eq. 8 and 9.

Table 1 shows infiltration rates and surface pressures measured in the test house with the ducts taped and untaped and with the furnace blower off.

Infiltration rates were measured by injecting a tracer gas into the house through a "spider" of four tubes arranged to distribute the gas throughout the house. The gas was mixed using either the furnace blower if the ducts were open, or desk fans if the ducts were taped closed. After mixing, the blower or fans were turned off and the concentration was measured using a four port sampling system which produces a coarse average of the concentration from different locations in the house.

Figures 5a and 5b are graphs of the data of Table 1. The solid lines in the graphs are the predictions of the simple models described by Eq. 8 and 9. The dashed lines are the fits of the measured data (assuming also that the air exchange rate is zero when the average surface pressure is zero). The agreement between the simple model and the measurements is surprisingly good. Let us emphasize that we have predicted infiltration rates for the house knowing only the average absolute value of the surface pressure on the shell and the total shell leakage. There are no undetermined parameters in this simple model.

While the results are encouraging, we acknowledge that many more measurements are necessary to adequately test the model. We shall discuss this further, below.

MULTI-CHAMBER MEASUREMENTS

Since the supply ducts pass through the crawl space and the return duct passes through the attic, large duct leakage in this house means that a flow coupling exists between the attic, the living space and the crawl space. Several authors have treated the multi-chamber infiltration theoretically (2-5). Because of its general importance we have begun measuring the flow coupling between spaces in this house.

Before describing the experiments to measure these flows we shall review Sherman's theory from the paper of Condon, et al. (2) applied to this particular example. The symbols used to describe the air flow for this case are shown in Fig. 6a. Note that the R's, the flow rates between volumes, are negative numbers. This implies that $-R_{ij}$ (when $i \neq j$), the flow of air from room j to room i, is a positive quantity. While this notation appears cumbersome, it simplifies the mathematics that follows. We define six air flow rates into and out of each of the three chambers. We do not assume that $R_{ij} = R_{ji}$ but from flow continuity the sum of the flows into a chamber is equal to the sum of flows leaving. Thus for the living space (space 1)

$$R_{01} + R_{21} + R_{31} = R_{10} + R_{12} + R_{13}. \quad (11)$$

We now define the total air flow into volume i to be

$$+ R_{ii} \equiv - \sum_{j=0}^3 R_{ij} \quad (i \neq j). \quad (12)$$

Thus, for volume 1 (the living space), the total air flow is

$$R_{11} = -R_{10} - R_{12} - R_{13} \quad (13)$$

and from (11) we have a second equality, $R_{11} = -R_{01} - R_{21} - R_{31}$. This definition makes the R_{ii} terms positive numbers.

We use a tracer gas to probe the structure to find the air flows, R_{ij} . A constant flow of tracer gas is injected into one or more of the volumes. When the concentrations in the three volumes approach equilibrium, these steady-state values are recorded and are used in the calculations described below.

Let F_k be the flow rate of tracer gas into one of the volumes (e.g., volume V_k) and C_i be the concentration in the i^{th} volume. The total flow of tracer into volume K is the sum of the tracer injection F_k and the tracer carried from other volumes. Thus

$$\text{Tracer flow into } K = F_k - \sum_{i=1}^3 R_{ki} C_i \quad (i \neq k) \quad (C_o = 0). \quad (14)$$

The flow of tracer out of V_k is the product of the concentration C_k times the sum of the flows out of that volume or

$$\text{Flow out of } K = - \sum_{i=1}^3 R_{ik} C_k \quad (i \neq k). \quad (15)$$

Using the definition of total flow, Eq. 12, we see that the tracer flow out of V_k can be rewritten

$$R_{kk} C_k = - \sum_{i=0}^3 R_{ik} C_k \quad (i \neq k). \quad (16)$$

Equating the steady-state flows of tracer in and out gives

$$- \sum_{i=0}^3 R_{ik} C_k = R_{kk} C_k = F_k - \sum_{i=1}^3 R_{ki} C_i \quad (i \neq k) \quad (17)$$

or

$$F_k = \sum_{i=1}^3 R_{ki} C_i \quad (\text{ie including } R_{kk} C_k). \quad (18)$$

In the volume for which no injection occurs,

$$0 = \sum_{i=1}^3 R_{ji} C_i \quad (\text{including } R_{jj} C_j). \quad (19)$$

In the particular case being considered, we have twelve flow unknowns. Three are determined using the three definitions of total flow, Eq 12. The other nine are determined from Eq 18 using three independent injection sequences, e.g. $F_1, 0, 0; 0, F_2, 0$; etc. Figure 7 illustrates the injection sequences used. These were selected in an attempt to keep the concentrations in the three test spaces in a range that could be measured accurately using our analyzer.

EXPERIMENTAL DETAILS

Measurements of cross-flows in this house are difficult to make because of poor mixing within the attic and within the crawl space. In an attempt to minimize these difficulties, injection into each of the spaces was effected using a "spider" of four tubes with their four ports distributed around the volume. The injection flow was controlled manually; the flow rate was measured using a rotameter. Estimates of equilibrium concentrations expected in each of the volumes were made; initial large injections to achieve these concentrations were followed by a steady injection rate into two of the volumes. Concentrations in each of the volumes were monitored until steady state concentrations in each of the volumes were seen. Fig. 7 shows the time history of three injection sequences.

After three independent injection sequences we have nine equations for nine unknowns R_{ij} . Eq 18 can be restated as a matrix equation

$$\underline{\underline{R}} \cdot \underline{\underline{C}} = \underline{\underline{F}} \quad (20)$$

where $\underline{\underline{R}}$, $\underline{\underline{C}}$ and $\underline{\underline{F}}$ are each 3×3 matrices (cf. Appendix A).

Then

$$\underline{\underline{R}} \cdot \underline{\underline{C}} \cdot \underline{\underline{C}}^{-1} (= \underline{\underline{R}}) = \underline{\underline{F}} \cdot \underline{\underline{C}}^{-1} \quad (21)$$

Data obtained from a trial with the ducts unsealed and the furnace blower and the air conditioner in operation are given in Table 2. (Injection in this case did not occur in the ducts but through the "spider" into separate volumes).

INTERPRETATION OF FLOWS

The air flows between the three spaces and the outside are shown in the air flow matrix $\underline{\underline{R}}$ of Table 2 and in Fig. 6b. The only unambiguous infiltration rates that can be defined for this system are R_{ij}/V_i . The values for the three spaces are:

$$\begin{aligned} \text{House: } & 0.25 \text{ hr}^{-1} \\ \text{Attic: } & 2.2 \text{ hr}^{-1} \\ \text{Crawl Space: } & 3.9 \text{ hr}^{-1} \end{aligned}$$

Matrix $\underline{\underline{\delta C}}$ in Table 2 is the error δC_{ij} of each element of $\underline{\underline{C}}$ and gives the standard deviation in the concentrations measured during the test. A description of matrix $\underline{\underline{\delta R}}$ is presented in Appendix B.

The physical sources of error are the result of imperfect mixing, the time variation of each R_{ij} and the random errors in the measurement of the concentration. A systematic error occurs because some of the injected tracer gas may leave the chamber without mixing with the gas in that chamber. This short circuiting would cause us to calculate too high a tracer flow in other chambers and too low a tracer flow in the injection chamber.

The time variation of the air flow rates, R_{ij} , can cause errors in the calculations. If any R_{ij} has an appreciable drift on the time scale of the entire set of measurements, a significant error can be introduced.

SUMMARY

We have reported a detailed study of infiltration rates measured with a tracer gas and air leakage rates obtained from fan pressurization in a small, three-bedroom California house. Surface pressure measurements are found to be an essential step in the process of finding a correlation between natural air infiltration and air leakage by pressurization. The surface pressure measurements reveal small pressures with a large fluctuating component. Directional effects of the wind are not seen; rather, the surface pressures are quite similar on all six faces of the living space parallelopiped. The measurement of the mean of the absolute value of the surface pressures, and the air leakage of the entire shell using fan pressurization permits estimating the natural infiltration rate of this structure. The estimate agrees well with measurements we have made.

Duct leakage is a major problem in this structure. It leads to significant cross flow between the attic, living space and crawl space. Attempts to measure these multi-chamber flows were complicated by poor mixing in the crawl space and were only partially successful.

Much remains to be done in order to model adequately the infiltration processes in this house. In particular, we must understand the relationship between the weather tower measurements and the structure of the surface pressures. In addition, we must develop a model to explain the effects of temperature differences on the infiltration that is seen. We have yet to determine if the stack effect is significant in this one-story house.

REFERENCES

1. Ross, H., Grimsrud, D. T., "Air Infiltration in Buildings: Literature Survey and Proposed Research Agenda," Department of Energy--Lawrence Berkeley Laboratory Report Number LBL-W7822, May 1978.
2. Condon, P. E., Grimsrud, D. T., Sherman, M. H., Kammerud, R. C., "An Automated Controlled-Flow Air Infiltration Measurement System," Proceedings of the ASTM Symposium on Air Infiltration and Air Change Rate Measurements, Washington, March 1978 (to be published). LBL Report Number 6849.
3. Honma, H., Ventilation of Dwellings and Its Disturbances. (Stockholm, Faibo Grafiska, 1975)

4. Sinden, F. W., "Multi-Chamber Theory of Air Infiltration," Building and Environment 1978, 13: 21-28.
5. Dick, J. B., "Experimental Studies in Natural Ventilation of Houses," J. Inst. Heat. Vent. Eng. 1949; 17:420-466.

ACKNOWLEDGEMENTS

The authors are indebted to the tireless support of David Krinkel who aided us in making measurements. We also thank John Janssen of Honeywell, Inc. for help in understanding the importance of the duct leakage in this house; Robert Socolow of Princeton University and Robert Sonderegger of LBL for stimulating ideas and discussions. Finally, we thank Howard Ross of the Department of Energy for patience and encouragement in supporting this research.

TABLE 1

INFILTRATION (MEASURED WITH TRACER GAS) VS. AVERAGE SURFACE PRESSURE MEASUREMENTS.
DATA PLOTTED IN FIG. 5

Duct Condition	Infiltration Rate (hr^{-1})	Average Negative Surface Pressure (Pa)	Average Positive Surface Pressure (Pa)	Average Surface Pressure (Pa)
Closed (Fig. 5a)	0.18	-0.34	+0.34	0.34
Closed	0.11	-0.27	+0.23	0.25
Cosed	0.18	-0.27	+0.28	0.28
Closed	0.13	-0.22	+0.26	0.25
Closed	0.16	-0.32	+0.25	0.28
Open (Fig. 5b)	0.28	-0.37	+0.29	0.33
Open	0.20	-0.26	+0.22	0.24
Open	0.23	-0.26	+0.29	0.27
Open	0.05	-0.07	+0.22	0.14
Open	0.28	-0.35	+0.25	0.30

TABLE 2

Multi Chamber Flow Results. For $\underline{\underline{F}}$ and $\underline{\underline{\delta R}}$ subscripts refer to volumes 1, 2 and 3 and off diagonal elements are shown in Fig. 6b. For $\underline{\underline{F}}$, $\underline{\underline{C}}$, and $\underline{\underline{\delta C}}$, the first subscript refers to space 1, 2 or 3 while the second to the experiment number as sketched in Fig. 7a, 7b or 7c.

$$\begin{aligned}
 \underline{\underline{F}} &= \begin{pmatrix} 0 & 33 & 33 \\ 47 & 0 & 94 \\ 142 & 142 & 0 \end{pmatrix} \text{ (cm}^3/\text{min)} \\
 \underline{\underline{C}} &= \begin{pmatrix} 24.8 & 27.6 & 31.1 \\ 38.9 & 4.7 & 14.4 \\ 40.0 & 28.9 & 11.8 \end{pmatrix} \text{ (ppm)} \\
 \underline{\underline{\delta C}} &= \begin{pmatrix} 0.4 & 0.7 & 0.6 \\ 6.4 & 0.5 & 3.1 \\ 11.0 & 9.3 & 1.0 \end{pmatrix} \text{ (ppm)} \\
 \underline{\underline{R}} &= \begin{pmatrix} 58 & -7 & -109 \\ 14 & 183 & -55 \\ 64 & -251 & 240 \end{pmatrix} \text{ (m}^3/\text{hr)} \\
 \underline{\underline{\delta R}} &= \begin{pmatrix} 31 & 42 & 72 \\ 25 & 30 & 81 \\ 71 & 95 & 180 \end{pmatrix} \text{ (m}^3/\text{hr)}
 \end{aligned}$$

APPENDIX A

Eq (18) represents a system of three equations in nine unknowns. These are

$$\begin{aligned} F_1 &= R_{11}C_1 + R_{12}C_2 + R_{13}C_3 \\ F_2 &= R_{21}C_1 + R_{22}C_2 + R_{23}C_3 \\ F_3 &= R_{31}C_1 + R_{32}C_2 + R_{33}C_3 \end{aligned} \quad (\text{A.1})$$

F_1 , F_2 and F_3 are controlled in an experiment; C_1 , C_2 and C_3 are measured. We wish to find the flows, R_{ij} . Eq (A.1) can be written in matrix form as

$$\begin{pmatrix} F_1 \\ F_2 \\ F_3 \end{pmatrix} = \begin{pmatrix} R_{11} & R_{12} & R_{13} \\ R_{21} & R_{22} & R_{23} \\ R_{31} & R_{32} & R_{33} \end{pmatrix} \begin{pmatrix} C_1 \\ C_2 \\ C_3 \end{pmatrix}. \quad (\text{A.2})$$

We define \underline{F} as the column vector of flows, \underline{C} as the column vector of concentrations and $\underline{\underline{R}}$ as the airflow matrix (the number of underscores indicates the dimensionality of the matrix). Eq (A.2) then becomes

$$\underline{F} = \underline{\underline{R}} \cdot \underline{C} \quad (\text{A.3})$$

The system of equations described above is undetermined. However if three sets of independent measurements are made and if the airflow matrix $\underline{\underline{R}}$ remains constant, the system is fully determined. The three sets of measurements can be written

$$F_1 = \underline{\underline{R}} \cdot \underline{C}_1 \quad F_2 = \underline{\underline{R}} \cdot \underline{C}_2 \quad F_3 = \underline{\underline{R}} \cdot \underline{C}_3 \quad (\text{A.4})$$

Since the three equations use the same matrix $\underline{\underline{R}}$ they can be rewritten

$$\begin{pmatrix} F_{11} & F_{12} & F_{13} \\ F_{21} & F_{22} & F_{23} \\ F_{31} & F_{32} & F_{33} \end{pmatrix} = \begin{pmatrix} R_{11} & R_{12} & R_{13} \\ R_{21} & R_{22} & R_{23} \\ R_{31} & R_{32} & R_{33} \end{pmatrix} \begin{pmatrix} C_{11} & C_{12} & C_{13} \\ C_{21} & C_{22} & C_{23} \\ C_{31} & C_{32} & C_{33} \end{pmatrix}. \quad (\text{A.5})$$

The first index denotes the chamber number and the second denotes the experiment number for the F 's and C 's. Defining the matrix of tracer flows as $\underline{\underline{F}}$ and the matrix of concentrations as $\underline{\underline{C}}$ we obtain Eq (20), ie

$$\underline{\underline{F}} = \underline{\underline{R}} \cdot \underline{\underline{C}} \quad (\text{A.6})$$

APPENDIX B

We assume (and from Fig. 7 the assumption seems reasonable) that the individual concentrations are uncorrelated. Then

$$\delta R_{ij} = \sqrt{\sum_{mn} \left(\frac{\partial R_{ij}}{\partial C_{mn}} \delta C_{mn} \right)^2} . \quad (B.1)$$

Define

$$\Delta_{ijmn} \equiv \frac{\partial R_{ij}}{\partial C_{mn}} . \quad (B.2)$$

We can find Δ_{ijmn} by differentiating equation (20) with respect to each concentration.

$$\frac{\partial F_{ij}}{\partial C_{mn}} = \sum_k \left(\frac{\partial R_{ik}}{\partial C_{mn}} C_{kl} + R_{ik} \frac{\partial C_{kl}}{\partial C_{mn}} \right) . \quad (B.3)$$

Since the F_{ij} 's are independent of C , the left side of eq (B.3) is zero. Further the C 's are uncorrelated so that

$$\frac{\partial C_{kl}}{\partial C_{mn}} = \delta_{km} \delta_{ln} . \quad (B.4)$$

Therefore

$$0 = \sum_k \frac{\partial R_{ik}}{\partial C_{mn}} C_{kl} + R_{ik} \delta_{km} \delta_{ln} . \quad (B.5)$$

Equivalently

$$\sum_k \Delta_{ikmn} C_{kl} = -R_{im} \delta_{ln} . \quad (B.6)$$

Multiplying by C_{lj}^{-1} and summing

$$\sum_{kl} \Delta_{ikmn} C_{kl} C_{lj}^{-1} = -\sum_l R_{im} \delta_{ln} C_{lj}^{-1}$$

Since

$$\sum_l C_{kl} C_{lj}^{-1} = \delta_{kj} , \text{ we have}$$

$$\Delta_{ijmn} = -R_{im} C_{nj}^{-1} \quad (B.7)$$

Finally we see that each individual term in the error matrix $\underline{\underline{\delta R}}$ can be found from the calculated flows and the inverted concentration

$$\delta R_{ij} = \sqrt{\sum_{m,n} (R_{im} C_{nj}^{-1} \delta C_{mn})^2} \quad (B.8)$$

Figure Captions

Fig. 1. Plan view of Walnut Creek House and its surrounding trees and fence.

Fig. 2. Air leakage as a function of indoor-outdoor pressure difference.

The solid line shows leakage with ducts open; the dashed line shows leakage with registers and furnace return duct taped.

Positive pressures indicate a higher pressure indoors than outdoors. $1 \text{ Pascal} = 1 \text{ N/m}^2 = \frac{1}{249} \text{ in. H}_2\text{O}$.

Fig. 3. Infiltration rates plotted as a function of wind speed measured on site. Indoor-outdoor temperature difference ($T_i - T_o$) ($^{\circ}\text{C}$) is indicated in parentheses next to each point.

Fig. 4a. The location of the wall pressure on the research house are shown by X. Numbers within the figure are the heights (in meters) of the taps above the ground. Numbers in parentheses are the 1-min averages of positive and negative pressure differences (in Pascals) at each pressure tap. The reference pressure in each case is the pressure within the living space.

Fig. 4b. The pressure measured on the south tap on the west side of the house plotted as a function of time. This trace is not coincident with the values recorded in Fig. 4a.

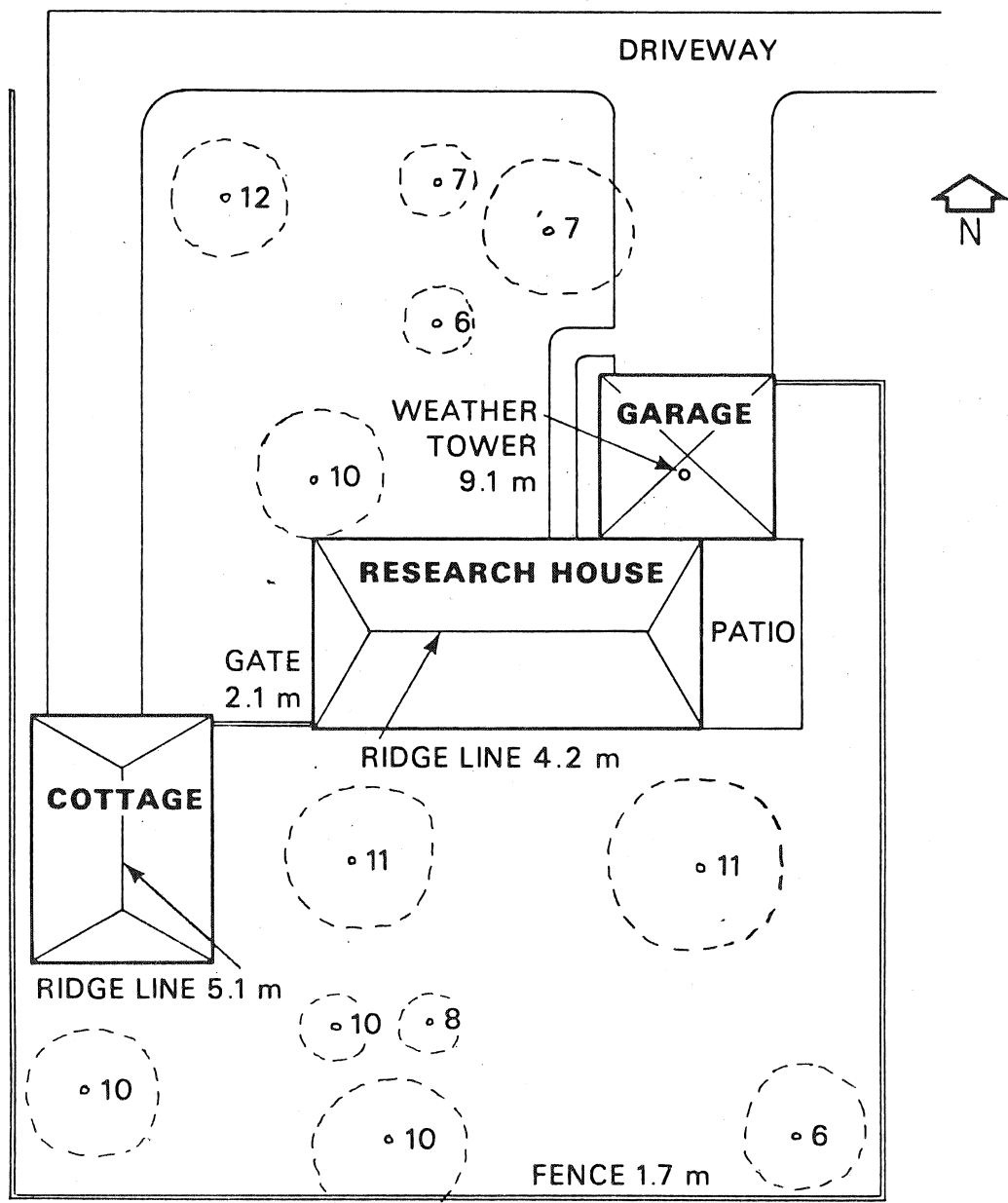
Fig. 5. Infiltration rates of Table 1 plotted as a function of the average surface pressure on the house. The solid line is the prediction of the simple infiltration model; the dashed line, the fit of the data.

Fig. 6a. Schematic representation of the air flows between the outside (subscript 0), living space (subscript 1), attic (subscript 2) and crawl space (subscript 3).

Fig. 6b. Flows of Table 2 measured between the three spaces and the outside. Flow units are (m^3 /hr). The volume of each of the spaces is indicated within the circles.

Fig. 7. Concentrations of Table 2 in the three spaces plotted as a function of time. In the top graph, gas was injected onto the attic and the crawl space; in the middle graph, into the crawl space and the house; and in the bottom graph, into the house and the attic. These are shown by asterisks in the figure.

0 5 10 10 Meters
0 10 20 30 Feet



(Numbers are height of trees in meters)

XBL 788-1537

Figure 1

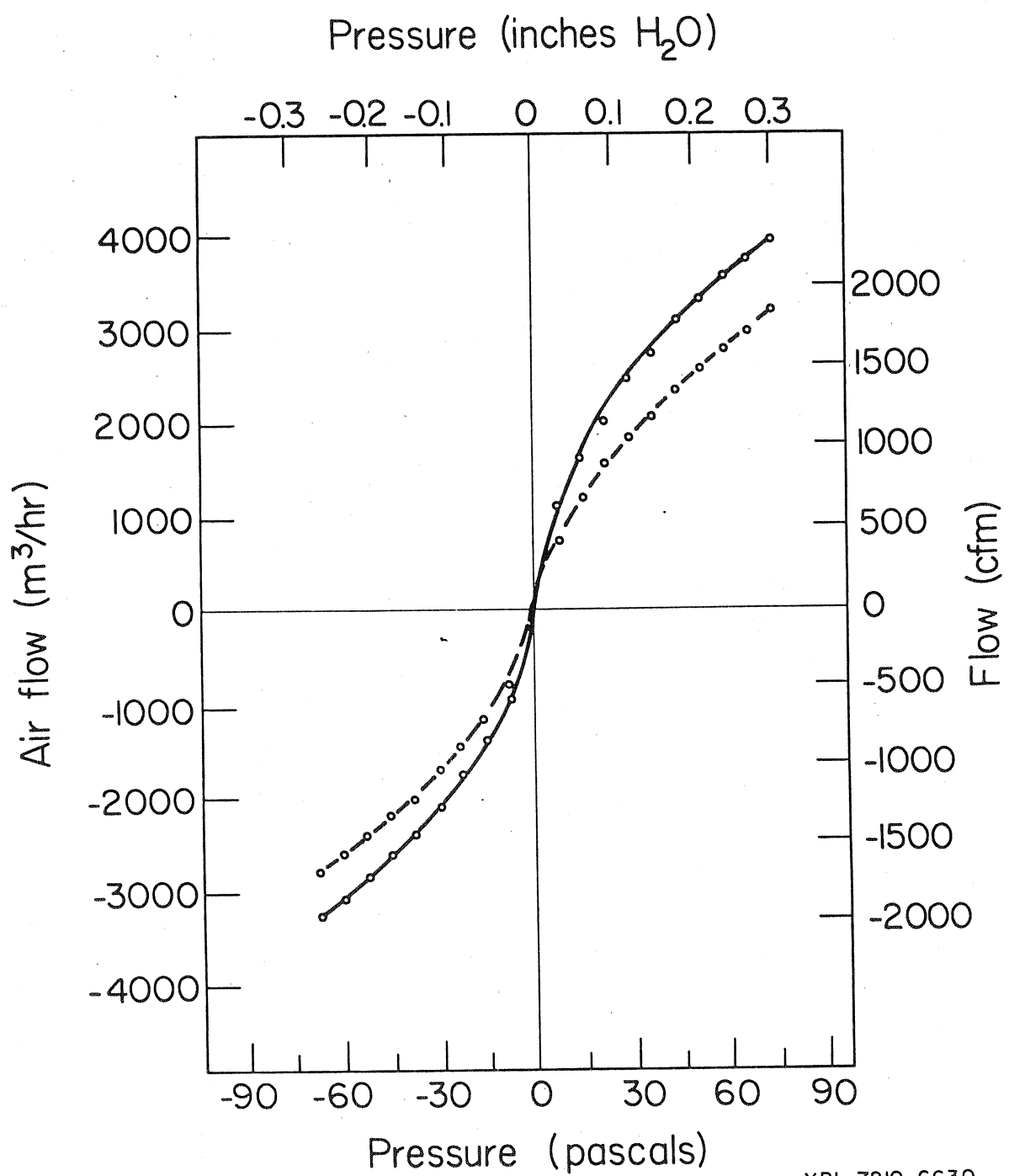
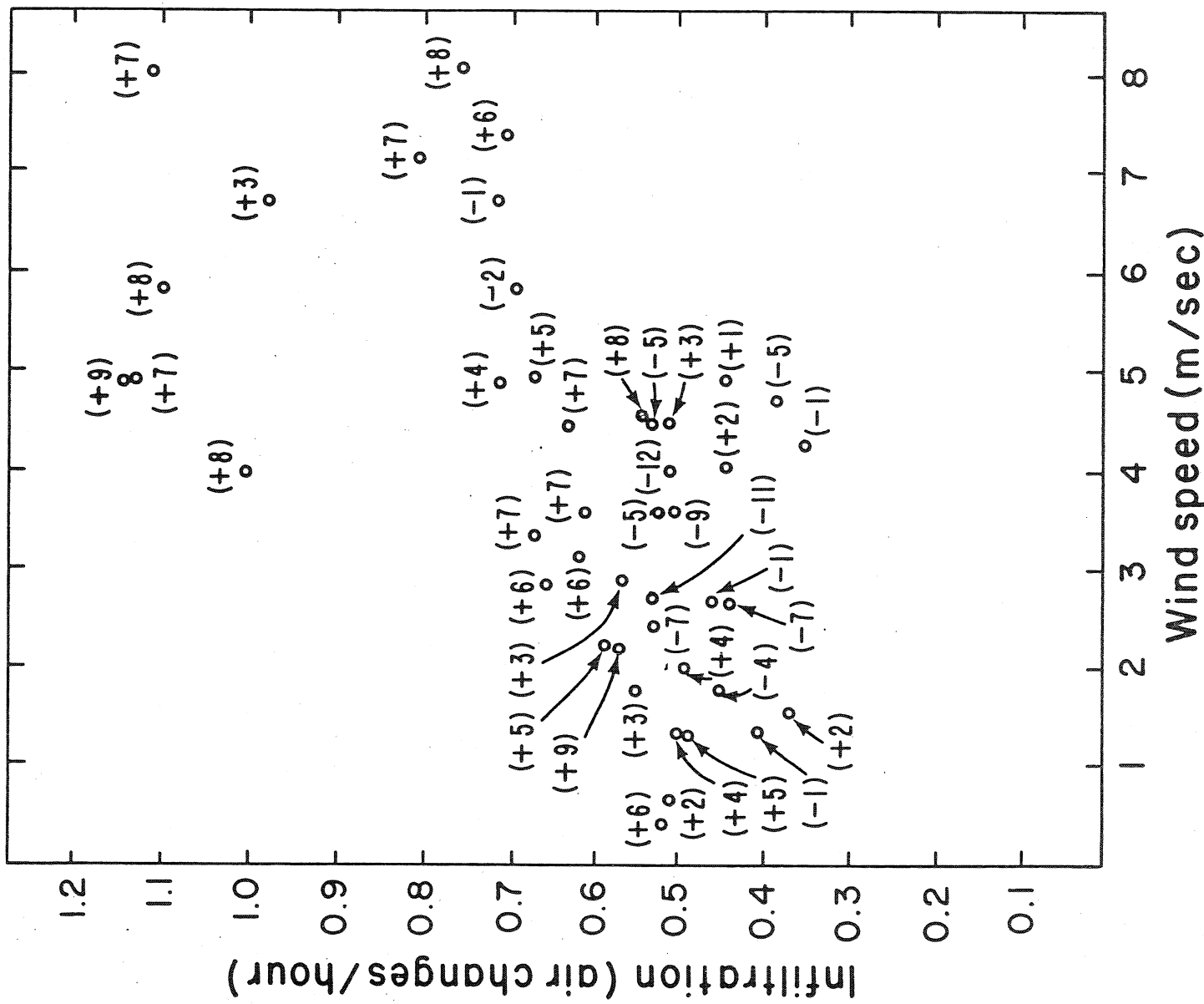


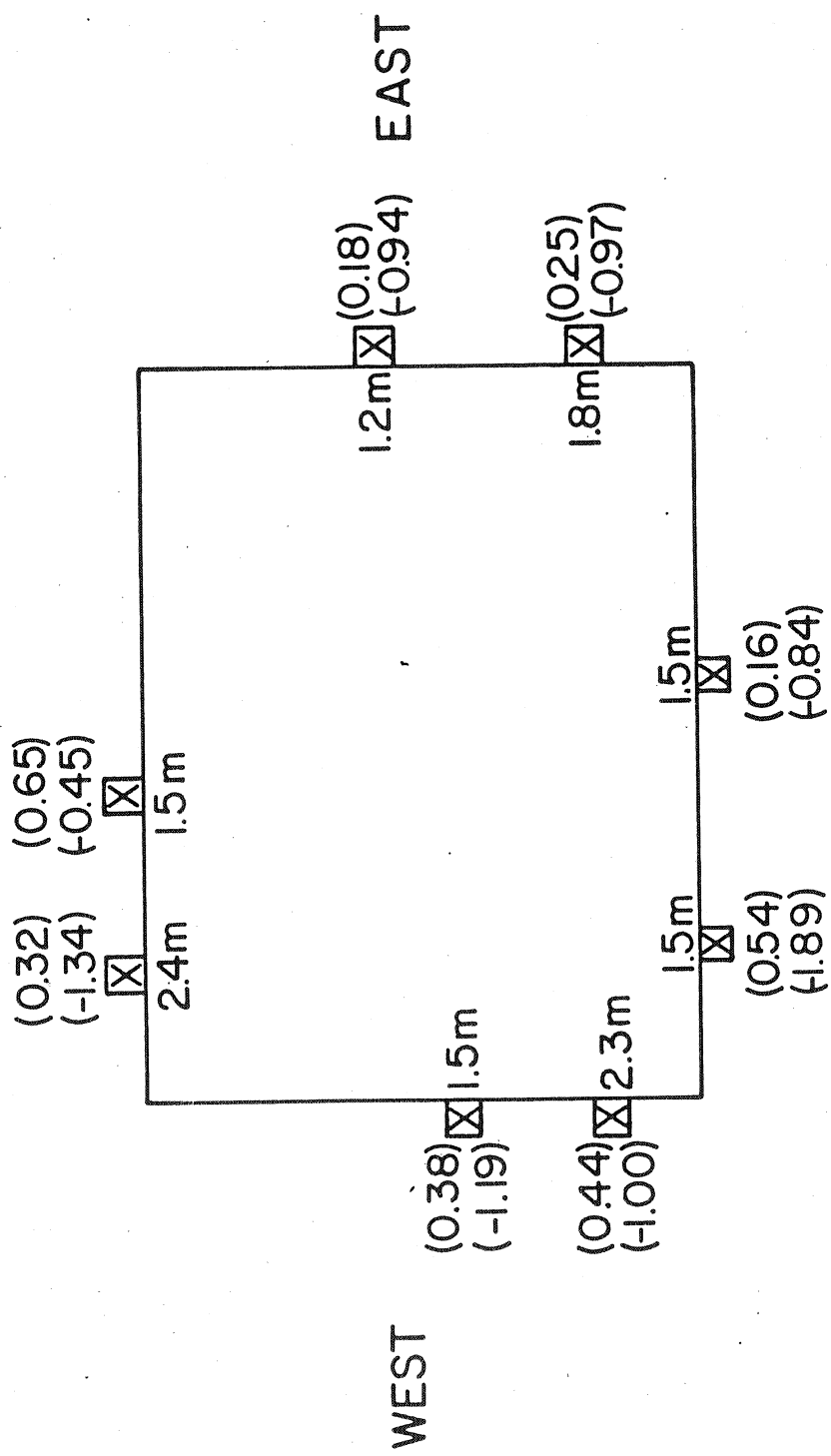
Figure 2



XBL 788-1539

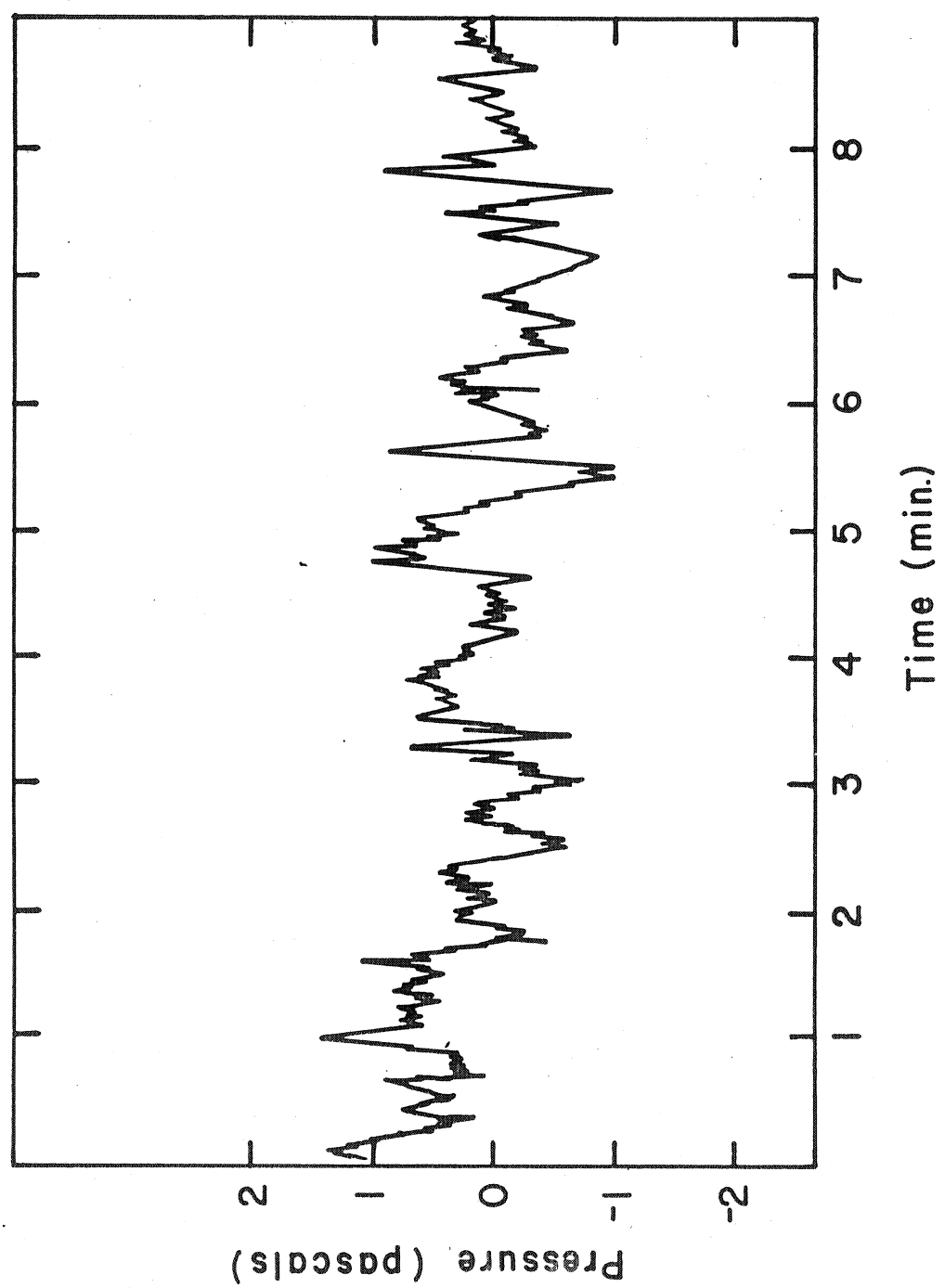
Figure 3

NORTH

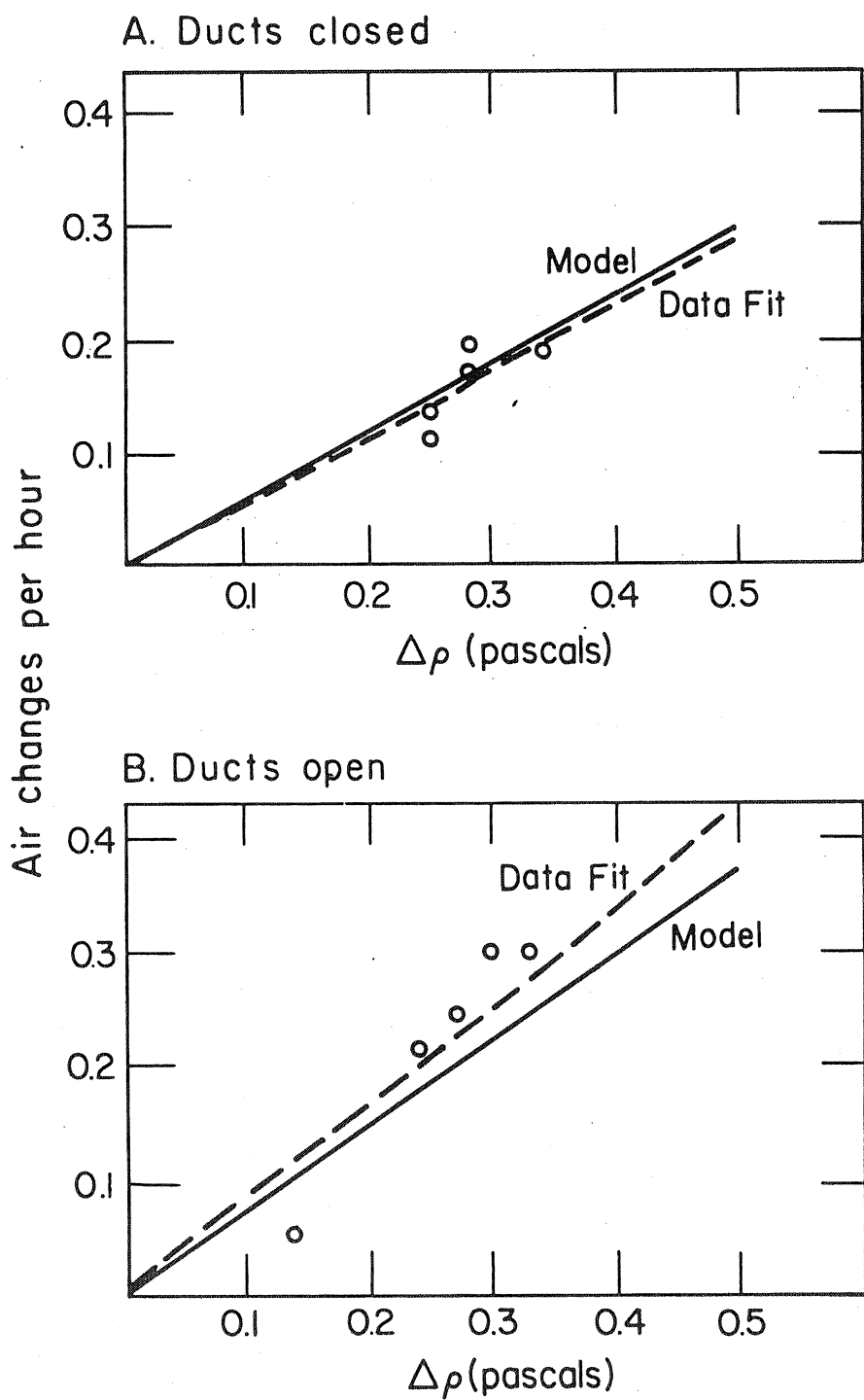


XBL 7810-6627

Figure 4a

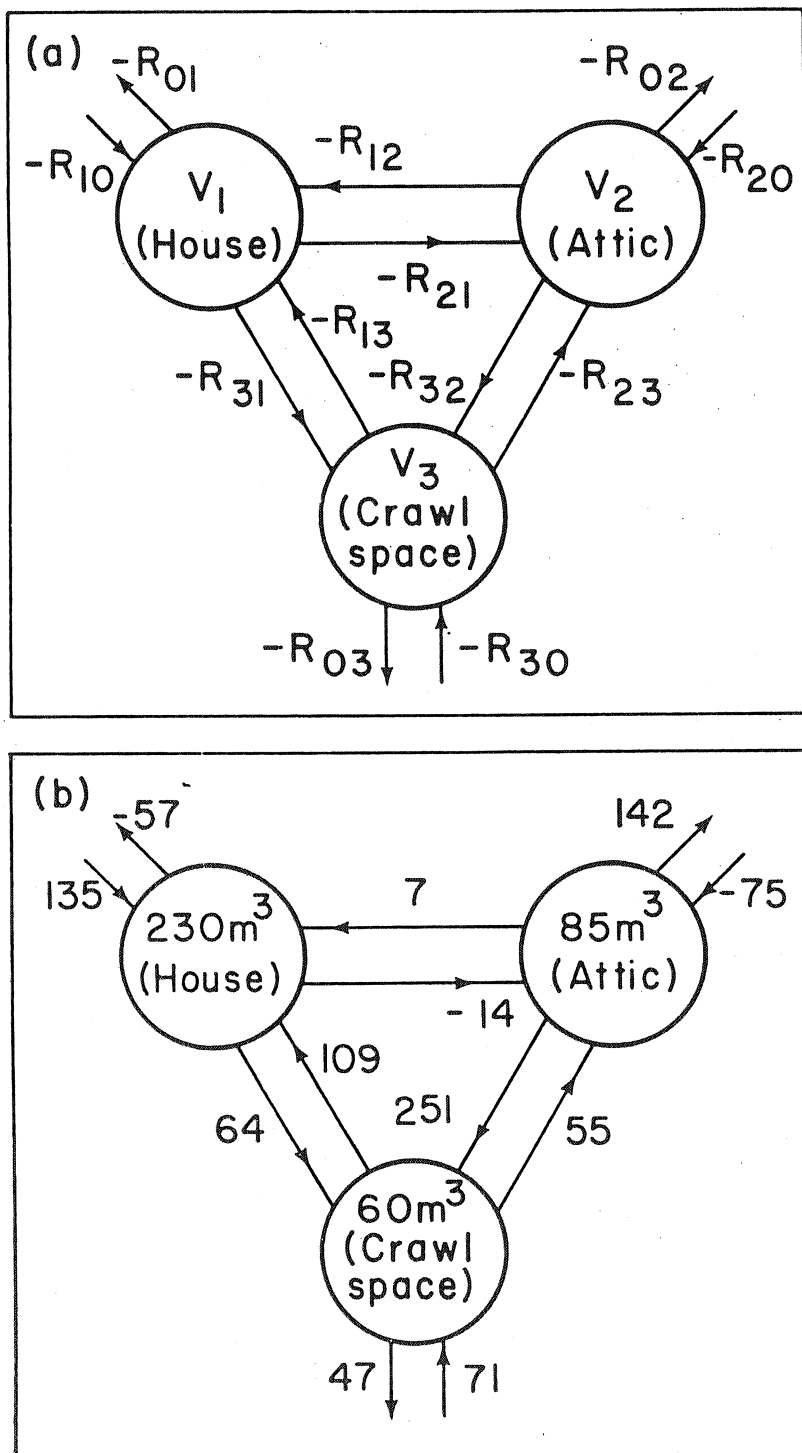


XBL 7810-6628



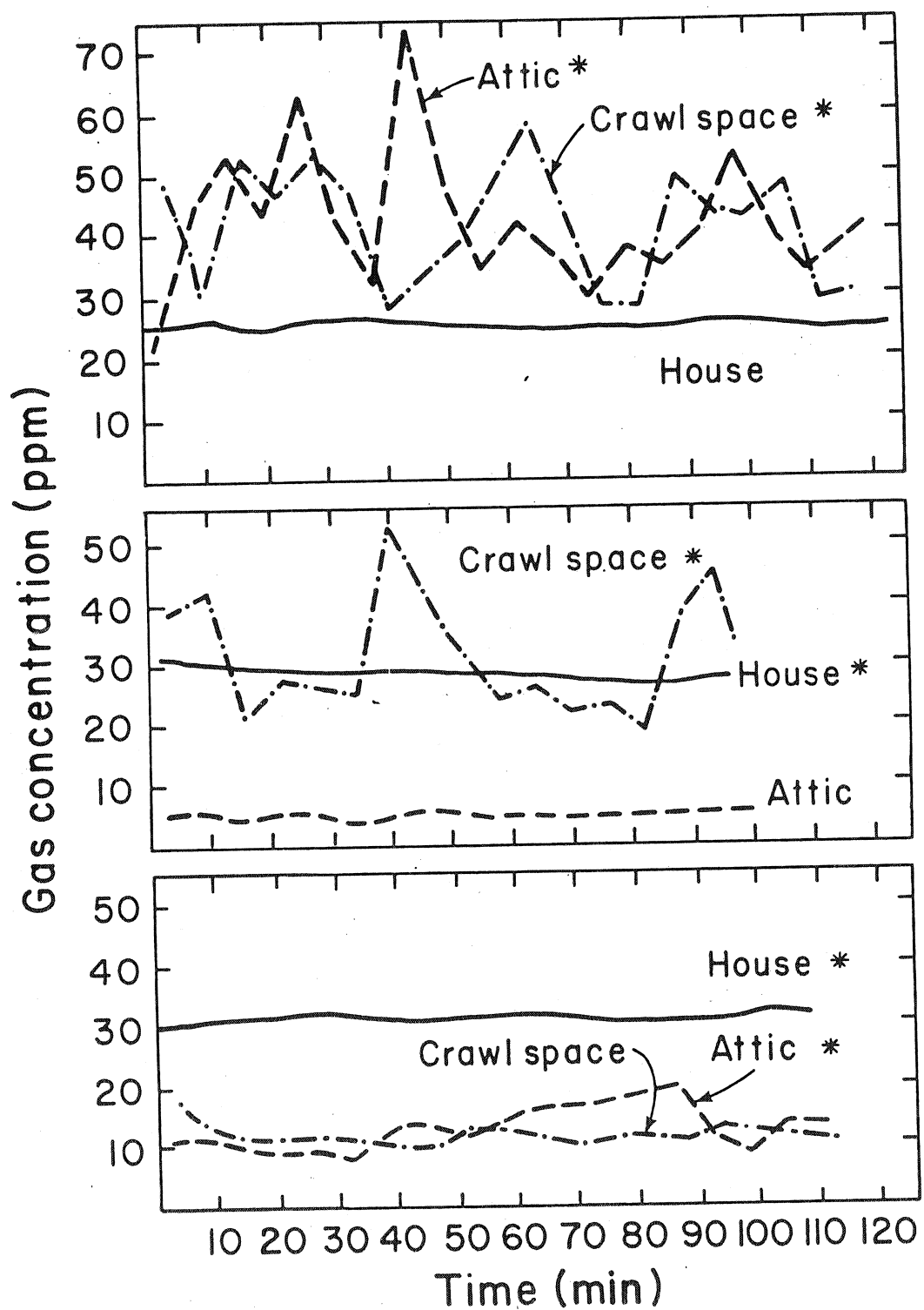
XBL 7810-6629

Figure 5a and 5b



XBL 788-1542

Figure 6a and 6b



XBL 788-1543

Figure 7a, 7b and 7c